Surface electronic structure study of Au/Si(111) reconstructions: Observation of a crystal-to-glass transition

H. M. Zhang,[1,*] T. Balasubramanian,[2] and R. I. G. Uhrberg[1]

[1]*Department of Physics and Measurement Technology, Linköping University, S-581 83 Linköping, Sweden*
[2]*MAX-lab, Lund University, Box 118, S-221 00 Lund, Sweden*

The α-$\sqrt{3}\times\sqrt{3}$, β-$\sqrt{3}\times\sqrt{3}$, and 6×6 surfaces of Au/Si(111) have been studied by angle-resolved photo-electron spectroscopy (ARPES). The α-$\sqrt{3}\times\sqrt{3}$ surface shows four surface state bands, one of which is a dispersing metallic band. Except for one nondispersing band near the Fermi level, the β-$\sqrt{3}\times\sqrt{3}$ surface shows surface bands that are similar to those of α-$\sqrt{3}\times\sqrt{3}$. Eight surface state bands have been found on the 6×6 surface instead of two as reported in the literature. Seven of these surface states are broadened into three, when the 6×6 phase is transformed into the quenched β-$\sqrt{3}\times\sqrt{3}$ phase just by annealing followed by quick cooling. The transition between the 6×6 and quenched β-$\sqrt{3}\times\sqrt{3}$ phases is consistent with a crystal-glass transition.

I. INTRODUCTION

A crystal-to-glass transition, which often occurs when a crystal is heated up to the liquid state and then quickly quenched to the solid state, is normally accompanied by a dramatic change of the electronic properties. In this study we report such a phenomenon in the two-dimensional Au/Si(111) system. It is well known that, when about one monolayer (ML) of Au is deposited on the Si(111) surface, several reconstructions, i.e., α-$\sqrt{3}\times\sqrt{3}$, β-$\sqrt{3}\times\sqrt{3}$, $2\sqrt{21}\times2\sqrt{21}$, $3\sqrt{3}\times3\sqrt{3}$, and 6×6 phases form depending on coverage and annealing.[1] In contrast to many other metal-induced superstructures on Si(111), Au/Si(111) surfaces contain significant structural disorder, that results in diffuse $\sqrt{3}$ spots in low-energy electron diffraction (LEED) patterns of the α-$\sqrt{3}\times\sqrt{3}$ phase, and ringlike diffraction in the case of β-$\sqrt{3}\times\sqrt{3}$. The $2\sqrt{21}\times2\sqrt{21}$ and 6×6 phases, on the other hand, show only sharp diffraction spots and are quite well ordered.

Unlike the Ag/Si(111) $\sqrt{3}\times\sqrt{3}$ surface, which is well described by the honeycomb-chain-trimer (HCT) model,[2] several controversial issues still remain for the Au/Si(111) $\sqrt{3}\times\sqrt{3}$ surface. No consensus has been obtained regarding the structure model or even Au coverage. One complicate factor is a significant amount of domain walls on the α-$\sqrt{3}\times\sqrt{3}$ and β-$\sqrt{3}\times\sqrt{3}$ phases, which inevitably overshadows the interpretation of experimental data and the comparison with structure models. In a previous theoretical study of the $\sqrt{3}\times\sqrt{3}$ surface, Ding *et al.* proposed the conjugate honeycomb chained trimer (CHCT) model with a nominal coverage of 1 ML for the Au/Si(111) $\sqrt{3}\times\sqrt{3}$ surface.[3] This model is related to the HCT model of the Ag/Si(111) $\sqrt{3}\times\sqrt{3}$ surface. The main difference between the CHCT and HCT models is that the metal trimers are arranged into a hexagonal pattern in the CHCT model instead of a honeycomb pattern as in the HCT model. Except for the Si trimers, the atomic structure of the CHCT model is similar to that of the inequivalent triangle (IET) model which was recently suggested for the low-temperature Ag/Si(111) $\sqrt{3}\times\sqrt{3}$ surface.[4] The Au/Si(111)

α-$\sqrt{3}\times\sqrt{3}$, β-$\sqrt{3}\times\sqrt{3}$, and 6×6 phases have been studied by scanning tunneling microscopy (STM) for many years.[5–8] It was concluded that the domain wall density of the $\sqrt{3}\times\sqrt{3}$ phase becomes higher as the Au coverage increases, and that crystallization of the domain wall structure results in the 6×6 phase at a Au coverage near 1 ML.[6,7] One interesting observation is that some empty state STM images of α-$\sqrt{3}\times\sqrt{3}$ also show a honeycomb pattern,[6,8] which suggests that the α-$\sqrt{3}\times\sqrt{3}$ and the Ag/Si(111) $\sqrt{3}\times\sqrt{3}$ surfaces have a similar structure. For the 6×6 phase, a pseudo-pentagonal glass model was proposed recently by Marks *et al.* based on surface x-ray diffraction data.[9,10] In this model, a network of incomplete pentagons and trimers form from the connection of every Au trimer with additional Au atoms.

From an earlier photoemission study, three surface state bands were reported on the $\sqrt{3}\times\sqrt{3}$ surface.[11] Later, Okuda *et al.* presented photoemission data of the α-$\sqrt{3}\times\sqrt{3}$, β-$\sqrt{3}\times\sqrt{3}$, and 6×6 surfaces.[12,13] Their valence band spectra showed a resemblance between the β-$\sqrt{3}\times\sqrt{3}$ and 6×6 surfaces,[13] that led to the conclusion that these surfaces have almost the same local structure in the area between the domain walls.

In this paper, the surface electronic structures of the α-$\sqrt{3}\times\sqrt{3}$, β-$\sqrt{3}\times\sqrt{3}$, and 6×6 surfaces have been investigated in detail by angle-resolved photoelectron spectroscopy. The α-$\sqrt{3}\times\sqrt{3}$ surface shows four dispersive surface state bands, three occupied and one partially occupied. Except for one broad, nondispersive surface state peak near the Fermi level (E_F), the β-$\sqrt{3}\times\sqrt{3}$ surface shows a surface electronic structure that is similar to the α-$\sqrt{3}\times\sqrt{3}$ phase. Interestingly, the 6×6 surface shows a lot of fine structure in the surface state region. Eight surface state bands are found in contrast to the two surface state bands reported in the previous study.[13] Seven of these surface states are broadened into three when the 6×6 phase is transformed to the quenched β-$\sqrt{3}\times\sqrt{3}$ phase by annealing followed by quick cooling. The electronic structures of these surfaces are discussed in comparison with the Ag/Si(111) phases.
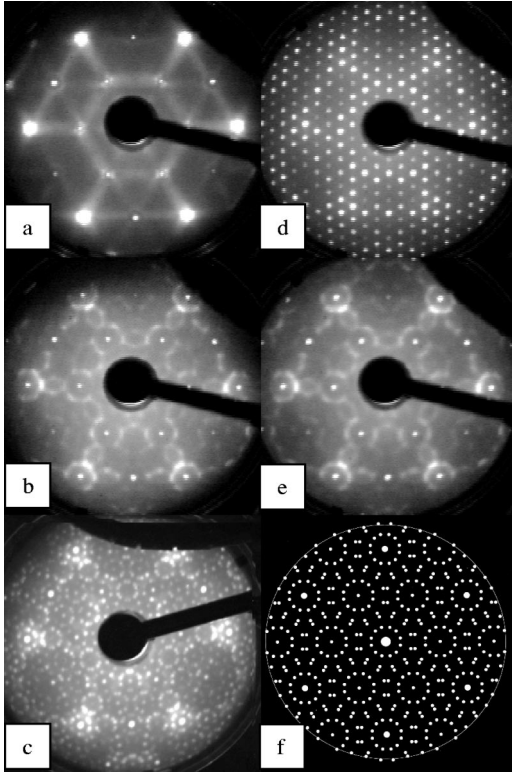
FIG. 1. LEED patterns of the Au/Si(111) surfaces as a function of Au coverage (100 K). (a) ~ 0.9 ML, α-$\sqrt{3}\times\sqrt{3}$ phase, 74 eV; (b) ~ 1.0 ML, β-$\sqrt{3}\times\sqrt{3}$ phase, 74 eV; (c) ~ 1.0 ML, $2\sqrt{21}\times 2\sqrt{21}$ phase, 74 eV; (d) ~ 1.1 ML, 6×6 phase, 74 eV; (e) ~ 1.1 ML, quenched β-$\sqrt{3}\times\sqrt{3}$ phase, 74 eV. (f) Schematic LEED pattern of the $\sqrt{39}\times\sqrt{39}$ phase.

II. EXPERIMENTAL DETAILS

The photoemission study was performed at beam line 33 at the Max-I synchrotron radiation facility in Lund, Sweden. The angle resolved valence band spectra presented here were obtained with a total energy resolution of ~ 50 meV with an angular resolution of $\pm 2°$. The pressure of the UHV system was around 4×10^{-10} Torr during the Au evaporation and 1×10^{-10} Torr during data collection. The Si(111) samples cut from a single crystal wafer (Sb doped, 3 Ω cm) were preoxidized by an etching method and cleaned *in situ* by stepwise direct current heating up to ~ 930 °C. This procedure resulted in a clean and well-ordered surface, as evidenced by the strong surface state emission and a sharp 7 $\times 7$ LEED pattern. Au was evaporated onto the Si(111) surface from a tungsten filament source calibrated by a quartz crystal monitor. Here, it is appropriate to consider the uncertainty in the Au coverage. An error on the order of 5–10 % is probably a realistic estimate. Evaporation of ~ 0.9 ML of Au followed by annealing at ~ 580 °C for 5 min. resulted in sharp $\sqrt{3}\times$ LEED spots surrounded by cloudlike diffraction [Fig. 1(a), α-$\sqrt{3}\times\sqrt{3}$]. The same annealing procedure of ~ 1.0 ML of Au resulted in sharp $\sqrt{3}\times$ LEED spots surrounded by ring-like diffraction [Fig. 1(b), β-$\sqrt{3}\times\sqrt{3}$]. However, the same annealing temperature and time, but ended by slow cooling to room temperature (RT), gave a new

$2\sqrt{21}\times 2\sqrt{21}$ LEED pattern [Fig. 1(c)]. Finally, ~ 1.1 ML of Au followed by annealing at ~ 700 °C for 1 min, and slow cooling to RT, led to the formation of a well-defined 6×6 LEED pattern [Fig. 1(d)]. Interestingly, the same annealing but ended by rapid cooling resulted in a quenched β-$\sqrt{3}\times\sqrt{3}$ LEED pattern [Fig. 1(e)]. A detailed inspection of the LEED images shows that the ringlike diffraction of the β-$\sqrt{3}\times\sqrt{3}$ phase resembles that of a $\sqrt{39}\times\sqrt{39}$ reconstruction [Fig. 1(f)], which has been observed for the Ag/Ge(111) system.[14] In other words, the β-$\sqrt{3}\times\sqrt{3}$ phase may be called a pseudo-$\sqrt{39}\times\sqrt{39}$ phase.

By measuring the total width of the valence band spectra ($h\nu = 21.2$ eV, -10 V sample bias), from the low energy cutoff to the Fermi level, we have determined the work function for the different surfaces. The values obtained for the 7×7, α-$\sqrt{3}\times\sqrt{3}$, β-$\sqrt{3}\times\sqrt{3}$, and 6×6 phases are 4.64, 5.19, 4.91, and 4.86 eV, respectively. The pinning position of the Fermi level with respect to the valence band maximum E_F-E_v was estimated by comparing bulk sensitive Si $2p$ core-level spectra obtained at a photon energy of 108 eV. Using a reference value of 0.63 eV for the Si(111)7$\times 7$ surface[15] we obtain E_F-E_v values of 0.13, 0.30, and 0.34 eV for the α-$\sqrt{3}\times\sqrt{3}$, β-$\sqrt{3}\times\sqrt{3}$, and 6×6 phases, respectively.

III. RESULTS AND DISCUSSION

To obtain the general picture of Au-induced surface reconstructions, it is worthwhile to compare Au/Si(111) to the closely related Ag/Si(111) and Ag/Ge(111) systems. The Ag/Si(111) and Ag/Ge(111) surfaces show almost the same surface reconstructions at coverages above 1 ML. The reconstructions change from $\sqrt{3}\times\sqrt{3}$ via $\sqrt{21}\times\sqrt{21}$ to 6×6 for Ag/Si(111) and from $\sqrt{3}\times\sqrt{3}$ via $\sqrt{39}\times\sqrt{39}$ to 6×6 for Ag/Ge(111) with increasing Ag coverage. Thus, it may not be too surprising that Au/Si(111) exhibits $2\sqrt{21}\times 2\sqrt{21}$ and 6×6 reconstructions and a $\sqrt{39}\times\sqrt{39}$-like periodicity at coverages around 1 ML. One interesting observation is that the LEED pattern of the β-$\sqrt{3}\times\sqrt{3}$ phase (~ 1.0 ML) is almost identical to the quenched β-$\sqrt{3}\times\sqrt{3}$ phase (~ 1.1 ML), although their corresponding well-ordered surfaces are the $2\sqrt{21}\times 2\sqrt{21}$ and 6×6 phases, respectively. This is consistent with STM observations that the β-$\sqrt{3}\times\sqrt{3}$ structure is actually quite similar to the $2\sqrt{21}\times 2\sqrt{21}$ and the 6×6 phases regarding the local atomic arrangement.[8] However, the most interesting phenomena are the transitions between the 6×6 and its quenched β-$\sqrt{3}\times\sqrt{3}$ phase and between the β-$\sqrt{3}\times\sqrt{3}$ and the $2\sqrt{21}\times 2\sqrt{21}$ phases. In this paper, we limit the discussion to the former case.

Figure 2 shows two sets of angle-resolved photoemission spectra from the α-$\sqrt{3}\times\sqrt{3}$ surface at low temperature (LT, 100 K) along the $\bar{\Gamma}$-$\bar{M}$-$\bar{\Gamma}$ line of the $\sqrt{3}\times\sqrt{3}$ surface Brillouin zone (SBZ) (see inset in Fig. 2). Four surface states were detected at both normal and 45° incidence angels and they are labeled S_1, S_2, S_3, and S_4. The α-$\sqrt{3}\times\sqrt{3}$ surface shows a clear metallic character, as evidenced by S_1 crossing
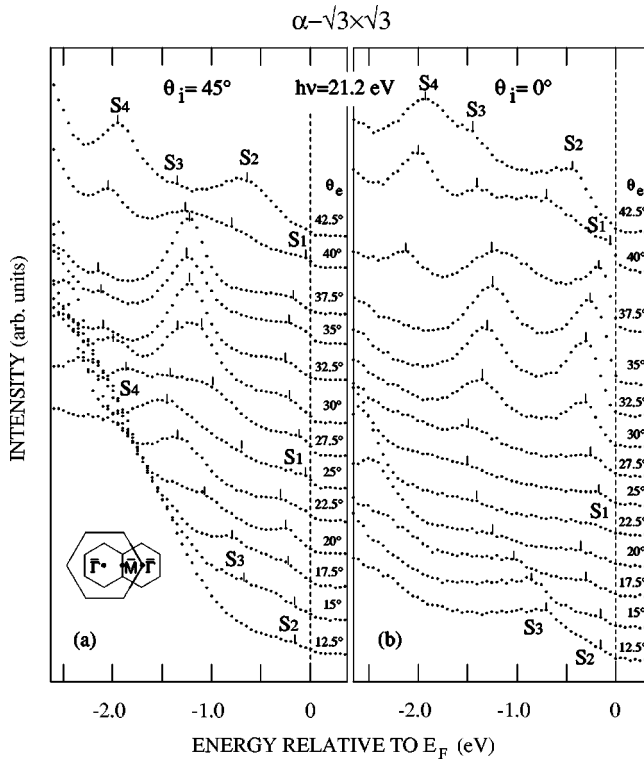
FIG. 2. ARPES spectra recorded from the Au/Si(111) α-$\sqrt{3}$ $\times \sqrt{3}$ surface with a photon energy of 21.2 eV at 100 K. The emission angles correspond to $\mathbf{k}_{\parallel}$ points throughout the first and second $\sqrt{3} \times \sqrt{3}$ SBZ, along the $\bar{\Gamma}$-$\bar{M}$-$\bar{\Gamma}$ line (see inset). (a) 45° incidence; (b) normal incidence. Four surface state bands are indicated by the labels S_1–S_4.

the Fermi level at $\theta_e = 25°$ and $\theta_e = 40°$ in Fig. 2(a). This result is consistent with an earlier study of the Au/Si(111) $\sqrt{3} \times \sqrt{3}$ surface by Karlsson *et al.*,[11] except for a new state S_4, which we tentatively assign to a surface state since it lies in the projected bulk band gap for emission angles around the second $\bar{\Gamma}$ point of the $\sqrt{3} \times \sqrt{3}$ SBZ. The surface state S_1 is located at -0.1 eV below E_F at $\theta_e = 27.5°$, and it disperses downwards to a minimum energy of -0.3 eV at $\theta_e = 32.5°$ around the second $\bar{\Gamma}$ point. It then moves upwards to cross the Fermi level at $\theta_e = 40°$. The other two surface state bands, S_2 and S_3, become degenerate at an initial energy of -1.4 eV below E_F at $\theta_e = 32.5°$ around the second $\bar{\Gamma}$ point. The surface state S_2 is located about -0.1 eV below E_F at $\theta_e = 15°$ and it disperses steeply downwards to the second $\bar{\Gamma}$ point. Then it shows up again at two high emission angles, 40° and 42.5° with a steep dispersion. S_3 is located at an initial energy of -0.7 eV at $\theta_e = 12.5°$, and it disperses downwards to a minimum energy of -1.5 eV at $\theta_e = 25°$. After that, S_3 disperses upwards to the second $\bar{\Gamma}$ point and splits out from S_2 at higher emission angles, then disperses downwards again. Figure 3 shows the surface band dispersions in the $\bar{\Gamma}$-$\bar{M}$-$\bar{\Gamma}$ direction of the $\sqrt{3} \times \sqrt{3}$ SBZ. The behaviors of S_1, S_2 and S_3 are similar to the surface state bands which were found on the Ag/Si(111) $\sqrt{3} \times \sqrt{3}$ surface.[16]
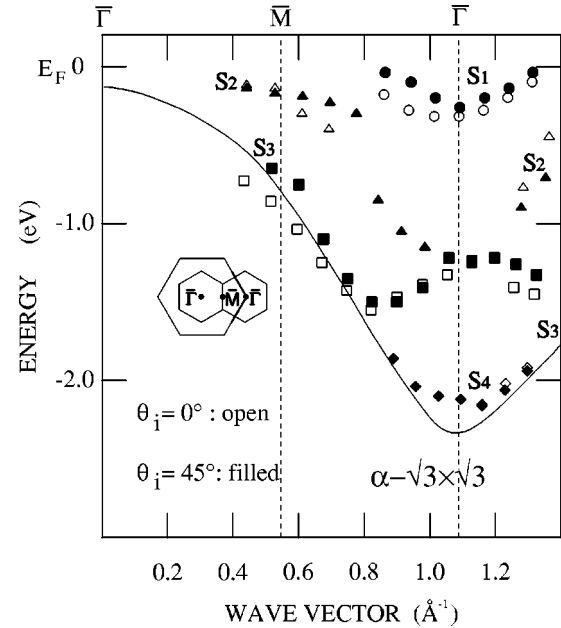
FIG. 3. Dispersions of the surface states from Fig. 2. Filled and open symbols correspond to 45° and normal incidence, respectively. The solid line shows the upper edge of the bulk bands projected onto the 1×1 SBZ.

From the Ag/Si(111) $\sqrt{3} \times \sqrt{3}$ surface, it is well-known that after the initial formation of the $\sqrt{3} \times \sqrt{3}$ surface there is always a strong partially occupied, dispersing surface state (S_1) near the Fermi level, even though the surface itself is intrinsically semiconducting.[16] The presence of S_1 on the Ag/Si(111) surface can be explained by extra Ag adatoms on the $\sqrt{3} \times \sqrt{3}$ surface.[16] A similar situation could apply to α-$\sqrt{3} \times \sqrt{3}$, i.e., the surface state band (S_1) is related to extra Au adatoms on the surface. The extra Au adatoms, which have loosely bound s electrons, lead to a partial occupation of an unoccupied surface state S_1 of the ideal $\sqrt{3} \times \sqrt{3}$ surface, resulting in a metallic α-$\sqrt{3} \times \sqrt{3}$ surface. In similarity with the Ag/Si(111) $\sqrt{3} \times \sqrt{3}$ case,[16] the Fermi pinning position for the Au/Si(111) α-$\sqrt{3} \times \sqrt{3}$ surface is also found around 0.1 eV above the valence band maximum. However, there is one significant difference between Au/Si(111) and Ag/Si(111). In the case of Ag/Si(111), S_2 and S_3 are located at higher binding energies near the $\bar{M}$ point of the $\sqrt{3} \times \sqrt{3}$ SBZ, while in the case of Au/Si(111), S_2 and S_3 have larger dispersions and are located near the Fermi level at lower emission angles. This will result in the different appearances in STM images of the Ag/Si(111) and Au/Si(111) surfaces. From theoretical calculations and earlier STM studies,[2,17] the honeycomb pattern of empty state images from the Ag/Si(111) $\sqrt{3} \times \sqrt{3}$ surface comes from the partially occupied surface state S_1. The existence of a quite similar partially occupied surface state (S_1) on Au/Si(111) α-$\sqrt{3} \times \sqrt{3}$ might be the reason why empty state images of this surface also shows a honeycomb pattern (at a certain bias). For the filled state STM images, in the Ag/Si(111) case, the main contribution still comes from S_1 within a 0.7 eV bias range, which naturally gives a honeycomb pattern. The situation in the
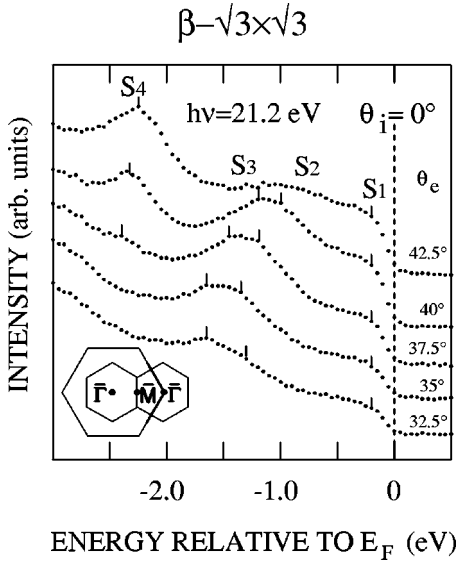
FIG. 4. ARPES spectra recorded from the Au/Si(111) β-$\sqrt{3}$ $\times \sqrt{3}$ surface with a photon energy of 21.2 eV at room temperature. The emission angles correspond to $\mathbf{k}_{\parallel}$ points in the second $\sqrt{3}$ $\times \sqrt{3}$ SBZ, along the $\bar{\Gamma}$-$\bar{M}$-$\bar{\Gamma}$ line (see inset).

Au/Si(111) case, on the other hand, becomes complicated since at biases $\gtrsim 0.1$ eV the tunnelling current also involves the contribution from the surface state S_2, resulting in a hexagonal appearance in the filled state STM images.[5,6] On the other hand, the difference in STM images may be also related to the intrinsic difference between the HCT and CHCT models.[2,3] In the HCT model, the metal trimers form a honeycomb pattern around Si trimers, while in the CHCT model, they form a hexagonal pattern, and the Si trimers show a honeycomb pattern around the metal trimers. To transform the HCT to the CHCT model, one way is to shrink all metal trimers separated by a $\sqrt{3} \times$ distance (and at the same time relax all Si trimers). This will create two possible $\sqrt{3} \times \sqrt{3}$ unit cells with a domain boundary since either of two neighboring metal trimers in a honeycomb arrangement can be shrank. The neighboring domains will have a phase shift of $1/\sqrt{3}$, which is exactly what happens on the Au/Si(111) α-$\sqrt{3} \times \sqrt{3}$ surface.[18] From earlier STM studies, an interesting observation is that a continuous deposition of either Ag or Au atoms on the Ag/Si(111) $\sqrt{3} \times \sqrt{3}$ surface transforms it into a $\sqrt{21} \times \sqrt{21}$ surface. It was concluded that the extra Ag or Au adatoms sit on top of Ag trimers instead of Si trimers.[19,20] The situation for Au/Si(111) might be quite similar, i.e., the extra Au adatoms on the α-$\sqrt{3} \times \sqrt{3}$ surface also sit on top of either of the two neighboring Au trimers in a HCT model, which induce a global modification of the HCT (honeycomb) configuration into two possible CHCT (hexagonal) arrangements. This explains the origin of domain walls on the α-$\sqrt{3} \times \sqrt{3}$ surface, i.e., the domain walls are actually domain boundaries between two possible $\sqrt{3} \times \sqrt{3}$ arrangements.[5–8] Thus the HCT instead of the CHCT model may be more suitable to describe the Au/Si(111) α-$\sqrt{3}$ $\times \sqrt{3}$ surface without extra Au adatoms.

Figure 4 shows a set of angle-resolved photoemission spectra from the room temperature β-$\sqrt{3} \times \sqrt{3}$ surface along the $\bar{\Gamma}$-$\bar{M}$-$\bar{\Gamma}$ line of the $\sqrt{3} \times \sqrt{3}$ SBZ. In accordance to LEED observations, the spectra of the β-$\sqrt{3} \times \sqrt{3}$ are essentially the same as those of the quenched β-$\sqrt{3} \times \sqrt{3}$ surface (here we only present the former). Near the Fermi level, a broad, nondispersive surface state peak (S_1) is very evident. Compared to α-$\sqrt{3} \times \sqrt{3}$, S_2 and S_3 of β-$\sqrt{3} \times \sqrt{3}$ also show a significant peak broadening. S_4, on the other hand, appears almost identical for the two surfaces. One major difference is that S_2, S_3 and S_4 are shifted downwards by approximately 0.2 eV when more Au atoms are deposited on α-$\sqrt{3} \times \sqrt{3}$ to form β-$\sqrt{3} \times \sqrt{3}$ (in other words, the Fermi position is lifted up with respect to the valence band maximum). This situation is similar to what happens when the $\sqrt{21} \times \sqrt{21}$ phase of Ag/Si(111) and the $\sqrt{39} \times \sqrt{39}$ phase of Ag/Ge(111) are formed by depositing more Ag onto the $\sqrt{3} \times \sqrt{3}$ surfaces.[14,21] In both the $\sqrt{21} \times \sqrt{21}$ and $\sqrt{39} \times \sqrt{39}$ cases, two surface state bands are found near the Fermi level. It is likely that the rather broad S_1 of β-$\sqrt{3} \times \sqrt{3}$ also contain more than one surface state band. To conclude this part, the general similarity between α-$\sqrt{3} \times \sqrt{3}$ and β-$\sqrt{3} \times \sqrt{3}$ comes from the common underlying $\sqrt{3} \times \sqrt{3}$ substrate while a further addition of Au adatoms gives the explanations for the downward shift and broadening of the surface states.

Interestingly, as shown in Fig. 5, eight surface state bands are found in the valence band spectra of the 6×6 phase, while only two surface state bands were reported in the previous study.[13] The sharp surface state peaks and the sharp LEED pattern clearly indicate a well-ordered 6×6 surface. Thus our photoemission data inevitably exclude the possibility of a β-$\sqrt{3}$-like 6×6 surface as reported in literature.[13] Recently, a pseudopentagonal glass model was proposed to describe the highly crystalline 6×6 surface based on surface x-ray diffraction data.[9,10] The glassy structures is, however, not consistent with the clear observations of the underlying $\sqrt{3} \times \sqrt{3}$ reconstruction by STM.[5,8] Figure 6 shows the surface band dispersions both in the $\bar{\Gamma}$-$\bar{K}$ and $\bar{\Gamma}$-$\bar{M}$ directions. In Fig. 5, the surface state band S_1' only shows up at some emission angles near the Fermi level. S_2', S_3', and S_4' appear "parallel" to each other and have small dispersions throughout the 1×1 SBZ in both directions. S_5' shows a certain dispersion in the $\bar{\Gamma}$-$\bar{K}$ direction and appears clearly at either higher or lower emission angles in the $\bar{\Gamma}$-$\bar{M}$ direction. Finally, the S_6', S_7', and S_8' surface states show up strongly in the $\bar{\Gamma}$-$\bar{K}$ direction at high emission angles. The increased number of surface state bands compared to the α-$\sqrt{3} \times \sqrt{3}$ surface may be caused by an adatom-induced surface band splitting. This is particularly evident in the Ag/Si(111) case. The initially-formed $\sqrt{3} \times \sqrt{3}$ surface of Ag/Si(111) has three surface state bands, which split into two groups of three surface bands each when extra Ag are added to the surface.[14,21] Such a splitting could explain the origin of the eight surface bands in the Au/Si(111) case. From our photoemission studies,[14,21] the two Ag-6×6 surfaces are semiconducting. For the Au-6×6 surface, we have not found any obvious, metallic character, which also indicates a possible semicon-
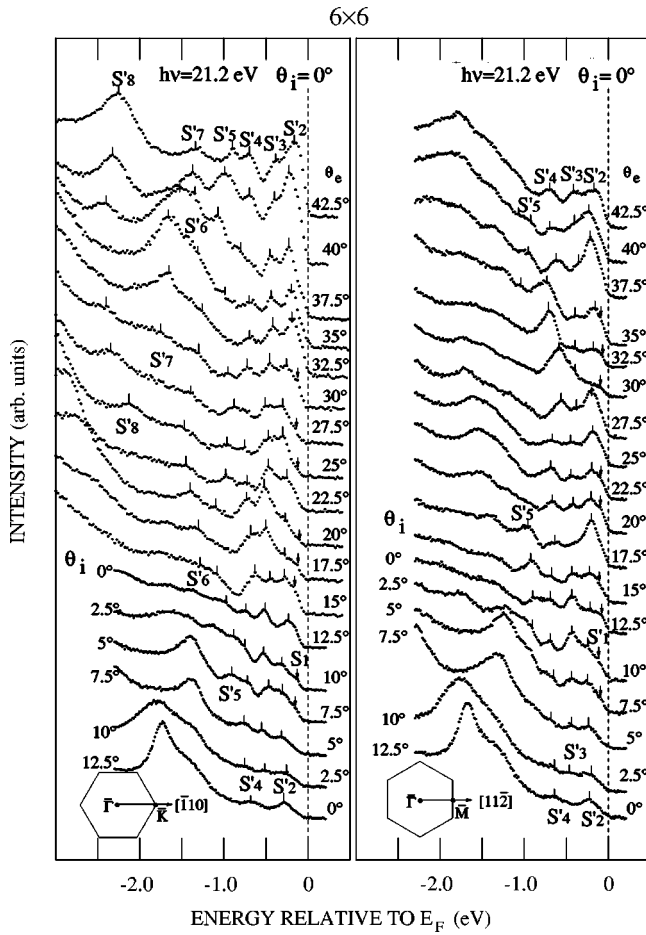
FIG. 5. Photoemission spectra recorded from the Au/Si(111) 6 ×6 surface, with a photon energy of 21.2 eV for various angles of emission along the $\bar{\Gamma}$-$\bar{K}$ and $\bar{\Gamma}$-$\bar{M}$ directions of the 1×1 SBZ at 100 K. Eight surface state bands clearly show up as S'_1–S'_8.

FIG. 6. Dispersions of the surface states along both the $\bar{\Gamma}$-$\bar{K}$ and $\bar{\Gamma}$-$\bar{M}$ directions of the 1×1 SBZ for the Au/Si(111) 6×6 surface. The dot size corresponds to the relative intensity of the different surface states. Solid and open circles are used to distinguish between the different surface state bands. The original spectra are shown in Fig. 5. The solid line shows the upper edge of the bulk bands projected onto the 1×1 SBZ.

ducting surface. Compared to the two Ag-6×6 surfaces, the Au/Si(111) one shows quite flat surface band dispersions near the Fermi level (see S_1 in Ref. 21).

An interesting thing happens when the 6×6 phase is heated up (becomes the well-ordered $\sqrt{3}\times\sqrt{3}$ phase) and is then quickly cooled down (becomes the quenched β-$\sqrt{3}$ $\times \sqrt{3}$ phase). Seven of the surface bands are washed out and appear as only three broad surface states. The result is opposite when a slow cooling process is applied after the annealing. Figure 7 shows the spectra from the α-$\sqrt{3}\times\sqrt{3}$, β-$\sqrt{3}$ $\times \sqrt{3}$, quenched β-$\sqrt{3}\times\sqrt{3}$, and 6×6 phases at $\theta_e=35°$. The dramatic change in the surface state bands is very evident when comparing Figs. 7(c) and 7(d). The quenched β-$\sqrt{3}\times\sqrt{3}$ phase with broadened surface states is obtained from the well-ordered crystalline 6×6 phase and depends very much on the annealing-cooling process. This clearly points to a disordered or rather a glasslike quenched β-$\sqrt{3}$ $\times \sqrt{3}$ phase as shown below. The β-$\sqrt{3}\times\sqrt{3}$ phase exists for Au coverages of ~1.0–1.1 ML with an approximate $\sqrt{39}\times$ distance in real space (close to 6×). At high temperature, all phases come from the same phase, that is the $\sqrt{3}\times\sqrt{3}$ + two-dimensional extra Au liquid (or gas). The beta phase is

just formed after quenching this phase, which does not critically depend on Au coverage, while slow cooling leads to different highly ordered phases depending on the precise Au coverage. This behavior resembles a crystal-glass (frozen liq-
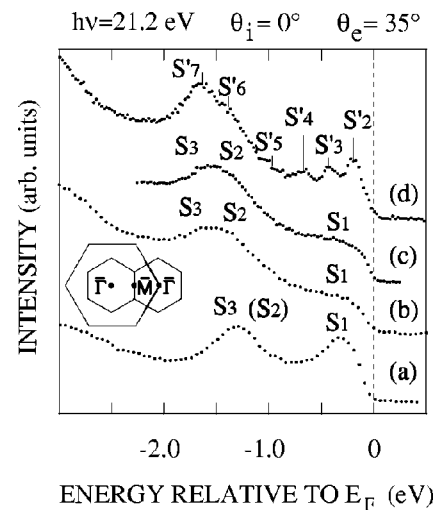
FIG. 7. Photoemission spectra recorded with a photon energy of 21.2 eV from different Au/Si(111) surfaces at 100 K. The spectra were recorded at an emission angle of 35° with normal light incidence (a) α-$\sqrt{3}\times\sqrt{3}$ phase; (b) β-$\sqrt{3}\times\sqrt{3}$ phase (c) quenched β-$\sqrt{3}\times\sqrt{3}$ phase; (d) 6×6 phase.

uid) transition in the bulk case. Thus the transformation between the 6×6 and quenched β-$\sqrt{3} \times \sqrt{3}$ phases is consistent with a crystal-glass transition.

The glasslike β-$\sqrt{3} \times \sqrt{3}$ phase can also be understood in terms of a "phase competition," since for similar Au coverages there exist at least three highly ordered phases ($3\sqrt{3} \times 3\sqrt{3}$, $2\sqrt{21} \times 2\sqrt{21}$, and 6×6).[1,5,8] From earlier STM studies,[5-8] the α-$\sqrt{3} \times \sqrt{3}$ and β-$\sqrt{3} \times \sqrt{3}$ surfaces are quite similar, except for a high domain wall density on the β-$\sqrt{3} \times \sqrt{3}$ surface. Also the β-$\sqrt{3} \times \sqrt{3}$ and 6×6 surfaces are quite similar, except for a crystalline order of the domain walls on the 6×6 surface. On the 6×6 surface, both RHEED and STM show the existence of an underlying $\sqrt{3} \times \sqrt{3}$ reconstruction.[5,8] Furthermore, at high temperature all surfaces show only the $\sqrt{3} \times \sqrt{3}$ reconstruction. It seems reasonable that these surfaces can be regarded as reconstructions caused by extra Au atoms sitting on the $\sqrt{3} \times \sqrt{3}$ substrate surface. Thus the differences between the α-$\sqrt{3} \times \sqrt{3}$, β-$\sqrt{3} \times \sqrt{3}$, 6×6, and the quenched β-$\sqrt{3} \times \sqrt{3}$ surfaces are the positions and the number of extra Au adatoms on the $\sqrt{3} \times \sqrt{3}$ surface (described by the HCT model). Similar situations have been observed on the $\sqrt{21} \times \sqrt{21}$ and 6×6 phases of Ag/Si(111), and $\sqrt{39} \times \sqrt{39}$ and 6×6 phases of Ag/Ge(111). From the STM images,[5,8] the extra Au atoms on the 6×6 surface are located to the Au trimer sites so that the honeycomblike $\sqrt{3} \times \sqrt{3}$ subunits still remain. If this is true, then the β-$\sqrt{3} \times \sqrt{3}$ surface could correspond to a disordered distribution of extra Au atoms. (There are two natural sites in the HCT model, i.e., the two neighboring Au trimer sites.) The domain wall areas of β-$\sqrt{3} \times \sqrt{3}$ could be those parts where the extra Au atoms are randomly distributed on either of two neighboring Au trimer sites. At high temperature, the extra Au atoms are highly mobile and they are not trapped by any specific site. Thus the surface shows a well-ordered $\sqrt{3} \times \sqrt{3}$ phase. When the temperature is slowly reduced, the extra Au atoms have enough time to find either of the two neighboring Au trimer sites and arrange themselves in a crystalline 6×6 periodicity. When the surface is quickly cooled, on the other hand, the extra Au atoms do not all find a proper Au trimer site, instead some of them may be trapped in a disordered fashion by the two Au trimer sites resulting in a glasslike, quenched β-$\sqrt{3} \times \sqrt{3}$ phase (pseudo-$\sqrt{39} \times \sqrt{39}$ phase).

IV. CONCLUSIONS

The surface electronic structures of four surfaces (α-$\sqrt{3} \times \sqrt{3}$, β-$\sqrt{3} \times \sqrt{3}$, 6×6, and quenched β-$\sqrt{3} \times \sqrt{3}$) have been investigated by ARPES. Four surface state bands are found on the α-$\sqrt{3} \times \sqrt{3}$ surface, one of which is a partially occupied surface state band (S_1). The electronic structure of the α-$\sqrt{3} \times \sqrt{3}$ shows a clear similarity with that of the Ag/Si(111) $\sqrt{3} \times \sqrt{3}$ surface. The β-$\sqrt{3} \times \sqrt{3}$ surface (or quenched one) shows four surface state bands with a broad surface state band (S_1) near the Fermi level. Eight surface state bands are found on the 6×6 surface in contrast to two as reported in an early study. Our photoemission data inevitably remove experimental support for a β-$\sqrt{3}$-like/glasslike 6×6 surface. Instead, the 6×6 surface is a highly ordered crystal phase. Seven of these surface states are broadened into three states, when the 6×6 phase is transformed into the quenched β-$\sqrt{3} \times \sqrt{3}$ phase. This behavior points to a crystal to glass transition between the 6×6 surface and the quenched β-$\sqrt{3} \times \sqrt{3}$ surface. The reconstructions of the β-$\sqrt{3} \times \sqrt{3}$ phase, the 6×6 and the quenched β-$\sqrt{3} \times \sqrt{3}$ phases have been explained in terms of extra Au adatoms on the $\sqrt{3} \times \sqrt{3}$ substrate described by the HCT model.

*Electronic address: hazha@ifm.liu.se

[1] C. Seifert, R. Hild, M. Horn-von Hoegen, R.A. Zhachuk, and B.Z. Olshanetsky, Surf. Sci. **488**, 233 (2001).

[2] See, for example, Y.G. Ding, C.T. Chan, and K.M. Ho, Phys. Rev. Lett. **67**, 1454 (1991); **69**, 2452 (1992).

[3] Y.G. Ding, C.T. Chan, and K.M. Ho, Surf. Sci. **275**, L691 (1992).

[4] H. Aizawa, M. Tsukada, N. Sato, and S. Hasegawa, Surf. Sci. **429**, L509 (1999).

[5] J. Nogami, A.A. Baski, and C.F. Quate, Phys. Rev. Lett. **65**, 1611 (1990); **65**, 2211 (1990).

[6] T. Nagao, S. Hasegawa, K. Tsuchie, S. Ino, C. Voges, G. Klos, H. Pfnür, and M. Henzler, Phys. Rev. B **57**, 10 100 (1998).

[7] T. Nagao, C. Voges, H. Pfnür, M. Henzler, S. Ino, F. Shimokoshi, and S. Hasegawa, Appl. Surf. Sci. **130/132**, 47 (1998).

[8] E.A. Khramtsova, H. Sakai, K. Hayashi, and A. Ichimiya, Surf. Sci. **433-435**, 405 (1999).

[9] L.D. Marks, D. Grozea, R. Feidenhans'l, M. Nielsen, and R.L. Johnson, Surf. Rev. Lett. **5**, 459 (1998).

[10] D. Grozea, E. Landree, L.D. Marks, R. Feidenhans'l, M. Nielsen, and R.L. Johnson, Surf. Sci. **418**, 32 (1998).

[11] C.J. Karlsson, E. Landemark, L.S.O. Johansson, and R.I.G. Uhrberg, Phys. Rev. B **42**, 9546 (1990).

[12] T. Okuda, H. Daimon, H. Shigeoka, S. Suga, T. Kinoshita, and A. Kakizaki, J. Electron Spectrosc. Relat. Phenom. **80**, 229 (1996).

[13] T. Okuda, H. Daimon, S. Suga, Y. Tezuka, and S. Ino, Appl. Surf. Sci. **121/122**, 89 (1997).

[14] H.M. Zhang, T. Balasubramanian, and R.I.G. Uhrberg, Phys. Rev. B **63**, 195402 (2001).

[15] F.J. Himpsel, G. Hollinger, and R.A. Pollak, Phys. Rev. B **28**, 7014 (1983).

[16] L.S.O. Johansson, E. Landemark, C.J. Karlsson, and R.I.G. Uhrberg, Phys. Rev. Lett. **63**, 2092 (1989); **69**, 2451 (1992).

[17] K.J. Wan, X.F. Lin, and J. Nogami, Phys. Rev. B **45**, 9509 (1992).

[18] T. Hasegawa, K. Takata, S. Hosaka, and S. Hosoki, J. Vac. Sci. Technol. A **8**, 241 (1990).

[19] J. Nogami, K.J. Wan, and X.F. Lin, Surf. Sci. **306**, 81 (1994).

[20] X. Tong, Y. Sugiura, T. Nagao, T. Takami, S. Takeda, S. Ino, and S. Hasegawa, Surf. Sci. **408**, 146 (1998).

[21] H.M. Zhang, K. Sakamoto, and R.I.G. Uhrberg, Phys. Rev. B **64**, 245421 (2001).